Food Chemistry 298 (2019) 125034

Contents lists available at ScienceDirect

Food Chemistry

journal homepage: www.elsevier.com/locate/foodchem

A wash-free and label-free colorimetric biosensor for naked-eye detection of aflatoxin B1 using G-quadruplex as the signal reporter

Jinghua Wu[a], Lingwen Zeng[a,b], Nianlong Li[a], Chengshuai Liu[c], Junhua Chen[d,*]

[a] School of Food Science and Engineering, Foshan University, Foshan 528000, China
[b] Institute of Environment and Food Safety, Wuhan Academy of Agricultural Science, Wuhan 430065, China
[c] State Key Laboratory of Environmental Geochemistry, Institute of Geochemistry, Chinese Academy of Sciences, Guiyang 550081, China
[d] Guangdong Key Laboratory of Integrated Agro-environmental Pollution Control and Management, Guangdong Institute of Eco-environmental Science & Technology, Guangzhou 510650, China

ARTICLE INFO

Keywords:
Aflatoxin B1
Visible biosensor
G-quadruplex
Signal amplification
Peanut samples

ABSTRACT

A wash-free and label-free colorimetric biosensor for the amplified detection of aflatoxin B1 (AFB1) has been constructed by the integration of an ingenious hairpin DNA probe with exonuclease III (Exo III)-assisted signal amplification. The presence of the AFB1 activates the continuous cleavage reactions by Exo III toward a hairpin probe, resulting in the autonomous accumulation of numerous free G-quadruplex sequences, which can catalyze the oxidation of 3,3′,5,5′-tetramethylbenzidine (TMB) by H_2O_2 to produce a colorimetric response. The naked-eye biosensor is ultrasensitive, enabling the visual detection of trace amounts of AFB1 as low as 1 pM without instrumentation. The sensor is robust and can work even when challenged with complex sample matrices such as peanut samples. With the advantages of simple operation, wash-free and label-free format, visible and intuitive output, and low cost, the naked-eye based colorimetric biosensor is expected to have potential applications for in-field detection of AFB1.

1. Introduction

Aflatoxin B1 (AFB1), the secondary metabolite of *Aspergillus flavus* and *Aspergillus parasiticus*, is the most predominant and toxic of mycotoxin that seriously threatens the health of humans and animals (Danesh et al., 2018). Many countries and regions have established regulations to govern the AFB1 level in agricultural products to guarantee food safety. For instance, the maximum permissible level of AFB1 set by the European Union is 2 ppb for groundnuts, milk, dried fruits, and cereals (Gilbert & Anklam, 2002). Thus, it is essential to develop sensitive and in-field detection techniques for AFB1 analysis to prevent exposure to the mycotoxin.

Conventional approaches included high-performance liquid chromatography (HPLC) and liquid chromatography-mass spectrometry (LC–MS) have been widely used for AFB1 detection (Eivazzadeh-Keihan, Pashazadeh, Hejazi, de la Guardia, & Mokhtarzadeh, 2017; Zhao, Huang, Ma, & Wang, 2017; Zitomer, Rybak, Li, Walters, & Holman, 2015). Although those methods provide satisfactory accuracy and sensitivity, they need expensive instruments, highly qualified technical staff, and cumbersome pretreatment steps, making them difficult to be used for on-site screening of AFB1. In recent years, a series of elegant sensing systems using antibody or aptamer as the molecular recognition element have been developed for AFB1 detection, including immunoassays (Lin, Zhou, Tang, Niessner, & Knopp, 2017; Wang et al., 2018; Zhang et al., 2014), electrochemical technique (Hao et al., 2017; Wang et al., 2018; Wu et al., 2017), and fluorescence detectors (Sabet, Hosseini, Khabbaz, Dadmehr, & Ganjali, 2017; Taghdisi, Danesh, Ramezani, & Abnous, 2018). Although significant contributions have been made to AFB1 detection, some of those methods often involve multiple incubation and washing steps and require specialized analytical instruments to get the output signals, which limit the on-site detection and point-of-use applications. As an alternative, colorimetric biosensors have been considered as promising sensing platforms for mycotoxin detection due to their advantages of cost-effectiveness, ease of use, and naked-eye readout (Chen, Wen, Zhuang, & Zhou, 2016; Ma et al., 2016; Shim, Kim, Mun, & Kim, 2014; Zhou et al., 2017). For example, Wang group (Hao, Lu, Zhou, Hua, & Wang, 2018) reported a pH-resolved colorimetric biosensor for AFB1 detection using malachite green carbinol base (MGCB) as the signal indicator. The AFB1 concentration can be obtained by adjusting the pH of the solution based on the combination of DNA-guided self-assembly of graphene oxide and magnetic separation. The detection limit of this colorimetric biosensor

* Corresponding author.
E-mail addresses: 222chenjunhua@163.com, jhchen@soil.gd.cn (J. Chen).

https://doi.org/10.1016/j.foodchem.2019.125034
Received 24 August 2018; Received in revised form 4 June 2019; Accepted 16 June 2019
Available online 17 June 2019

for AFB1 is 10 ng mL^{-1} (about 32 nM). Arduini and colleagues (Arduini et al., 2016) have designed a sensor for AFB1 detection using the acetylcholinesterase (AChE) enzyme that is inhibited by this toxin, and the degree of inhibition was quantified by the Ellman's spectrophotometric method, obtaining a detection limit of 10 μg L^{-1}. Hosseini, Khabbaz, Dadmehr, Ganjali, & Mohamadnejad (2015) have developed a colorimetric biosensor for the detection of AFB1 based on the interaction of gold nanoparticles (AuNPs) with the aptamer. The color change of AuNPs from red to purple can be used to detect the AFB1 concentration, with a detection limit of 7 nM. However, those colorimetric assay is often confronted with low detection sensitivity. Therefore, it is still highly necessary to develop a reliable sensor with amplified colorimetric signal for on-site detection of AFB1.

To achieve high sensitivity for mycotoxin detection, nuclease-assisted signal amplification strategy has been widely applied because of the excellent catalytic activity (Li et al., 2017; Lv, Li, Cui, Zhao, & Guo, 2017). Different of the characteristics of endonuclease, no any specific DNA sequence is required for exonuclease recognition, thus, it provides a universal tool for signal amplification (Wang, Yu, Han, Xie, & Chen, 2017; Wu, Xu, Jin, & Irudayaraj, 2018). With such unique advantages, Exo III has been successfully employed for amplified detection of DNA (Liu et al., 2014, 2015; Wang, Wang, Zhang, Tang, & Zhang, 2018), proteins (Chen, Ding, Song, Yang, & Ju, 2016; Lu, Su, & Li, 2017; Zhang et al., 2014), and metal ions (Wu, Zhang, Wang, Mi, & Sun, 2018; Xu, Gao, Wei, Chen, & Tang, 2016). To explore the new application of Exo III-mediated target detection, we developed a wash-free and label-free colorimetric biosensor for AFB1 detection using Exo III as the catalyst. Attempting to realize visual detection, G-quadruplex DNAzyme (Chen, Chen, & Li, 2017; Chen, Pan, & Chen, 2018; Chen, Zhou, & Wen, 2015; Huang et al., 2019; Jo, Mun, Kim, Shim, & Kim, 2016), which can effectively catalyze the H_2O_2-mediated oxidation of TMB to generate a color change, was used as the signal transducer.

2. Experimental section

2.1. Chemicals

AFB1, H_2O_2 (30 wt%), TMB, methanol, and Tris were ordered from Sigma-Aldrich (St. Louis, Mo). DMSO was used to prepare the hemin solution (5 mM) and stored at −20 °C. Exo III was obtained from New England biolabs (Ipswich, MA). Ultrapure water from a Milli-Q water purification system was used in all the experiments.

The DNA probes were ordered from Shanghai Sangon Biotechnology Co., Ltd. (Shanghai, China) and the specific sequences were shown as follows:

Aptamer: 5'-GTTGGGCACGTGTTGTCTCTCTGTGTCTCGTGCCCTTCGCTAGGCCC-3'

a*

DNA1: 5'-ACACAGAGAGAC-TTCAGA-3'

a* b a a

HP: 5'-ACACAGAGAGAC-AAGGGTAGGGCGGGTTGGGTT-GTCTCTCTGTGT-GTCTCTCTGTGT-3'

2.2. Analysis of AFB1 in buffer solution

Aptamer sequence (150 nM) in the reaction buffer (pH 7.4, 15 mM Tris-HCl, 100 mM NaCl, 10 mM KCl, and 10 mM $MgCl_2$) was incubated with DNA1 (150 nM) for 30 min. Then, AFB1 was added, and incubated for 40 min. Subsequently, HP (500 nM) and Exo III (2 units/μL) were mixed in the reaction buffer and stayed for 40 min. The experiment was carried out at room temperature. 40 μL of the above resulting solution was mixed with 10 μL of the hemin solution and incubated for 30 min. Then, 50 μL of the product was added into 950 μL of the TMB-H_2O_2 solution. The final mixture was incubated for 20 min and measured by a UV–vis spectrophotometer (UV-2600, Shimadzu).

Other mycotoxins including aflatoxin B2 (AFB2), aflatoxin M1 (AFM1), aflatoxin G1 (AFG1), aflatoxin G2 (AFG2), ochratoxin A (OTA), deoxynivalenol (DON), zearalenone (ZEN), and fumonisin (FB1) at 100 nM were also tested in the same way to assess the specificity of the assay.

2.3. Analysis of AFB1 in peanut samples

AFB1-free peanut samples were purchased from local market and finely milled by a household blender. 5 g of the blank peanut sample was spiked with different concentrations of AFB1 (0.1, 1, 10, 25, and 50 nM) and then extracted with methanol-water (30 mL, 8:2, v/v) under gentle stirring on a shaker for 40 min. The supernatant after centrifugation (5000 g, 10 min) was filtered through a 0.22 μm syringe filter and diluted 20-fold using the reaction buffer for recovery test. The detection step was the same as in the buffer solution.

3. Results and discussion

3.1. Design strategy for AFB1 detection

The design strategy of the wash-free and label-free colorimetric biosensor for naked-eye detection of AFB1 is schematically illustrated in Scheme 1. A hairpin DNA probe (HP) was designed, which contained a 3′-protruding segment (domain a) as the recognition unit, the stem region (domains a and a*), and a caged G-rich sequence located in the loop region (domain b). Domain a is complementary to domain a*. Without AFB1 in the sensing system, domain a* of DNA1 hybridized with the AFB1 aptamer, which prevented the further hybridization reaction between DNA1 and HP. Thus, HP with a protruding segment (domain a) at the 3′-terminus cannot be digested by Exo III due to the fact that Exo III only cleaves duplex DNA from blunt or recessed 3′ termini. In the presence of AFB1, the specific interaction between AFB1 and the aptamer sequence liberates DNA1 to bind with segment a of HP, leading HP to become a blunt 3′-terminus probe. Exo III thus can catalyze the cleavage of mononucleotides from this end, releasing DNA1 to participate for the next cyclic hybridization and digestion process (Cycle I). In addition, a new DNA fragment (domains a* and b) is also liberated, which could be used for the successive hybridization with HP. Following the cleavage reaction by Exo III, the new DNA fragment can be recycled to trigger the autocatalytic digestion of HP (Cycle II). Based on the autonomous cleavage reactions in Cycles I and II, the DNA fragment containing the G-rich sequence (domain b) can be exponentially released, leading to the cascade signal amplification for AFB1 monitoring. The released G-rich oligomer can fold into active DNAzyme with cofactor hemin. Then the G-quadruplex DNAzyme can catalyze the H_2O_2-mediated oxidation of the colorless TMB to the blue-colored TMB^+, which provides the amplified colorimetric signal for AFB1 detection.

3.2. Feasibility verification

To evaluate the feasibility of the colorimetric biosensor for naked-

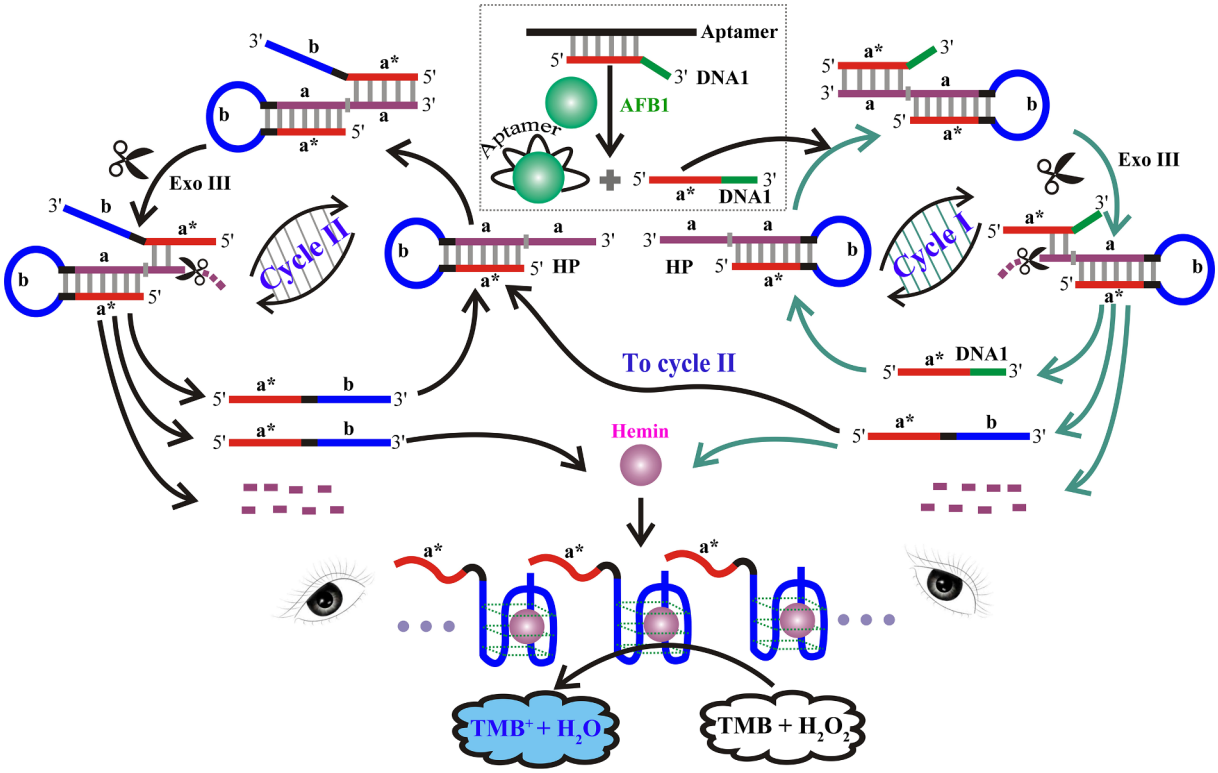

Scheme 1. Schematic illustration of the sensing strategy for AFB1 detection by the naked eye using G-quadruplex as the signal reporter. Domain a is complementary to domain a*. Domain b is the caged G-rich sequence. Exo III is used to perform the cyclic cleavage reactions in Cycles I and II.

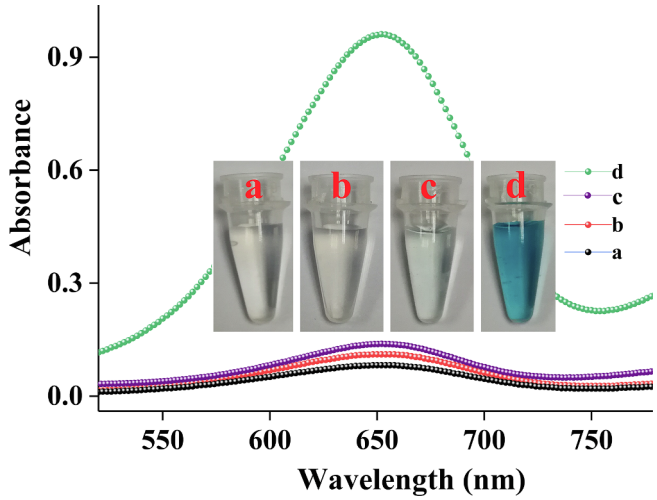

Fig. 1. UV–vis absorbance spectra of the test solution under different experimental conditions: (a) no AFB1, no Exo III, (b) 1 nM AFB1, no Exo III, (c) no AFB1, 2 unit/μL Exo III, and (d) 1 nM AFB1, 2 unit/μL Exo III. TMB-H_2O_2 reaction solution was used to obtain the colorimetric signals. Insets: The corresponding photographs of the naked-eye color difference. (For interpretation of the references to colour in this figure legend, the reader is referred to the web version of this article.)

eye detection of AFB1, the colorimetric response and absorption spectra were investigated in control tests. As depicted in Fig. 1, in the presence of AFB1 and Exo III, a readily detectable absorption peak at 650 nm could be observed (curve d). This peak could be attributed to the cyclic cleavage of the caged HP to release the G-rich sequence for the generation of numerous active G-quadruplex DNAzymes. However, in the case of no target AFB1 and Exo III, only a very low background signal can be detected (curve a). By the introduction of AFB1 without Exo III or in the presence of Exo III without AFB1, no obvious difference in the signal can be observed with the comparison of curve a (curves b and c). If the solution without target AFB1 or Exo III, The HP still keeps the hairpin structure and cannot be cleaved. Thus, the caged G-rich DNA fragment failed to release. The formation of active hemin/G-quadruplex DNAzyme was thus suppressed. The corresponding naked-eye observation of the color difference were shown in inset of Fig. 1. Those results clearly demonstrated the feasibility of our developed autocatalytic DNA circuit for target AFB1 detection.

3.3. Optimization of experimental parameters

In this study, the concentration of Exo III plays a significant role in the signal amplification process. As shown in Fig. 2A, 2 unit/μL of Exo III can provide the best signal-to-noise (*S/N*) ratio. At the higher concentration of Exo III, the *S/N* decreased, which might be attributed to the non-specific cleavage toward HP without AFB1, yielding a high background signal. Therefore, 2 unit/μL of Exo III was used in the following study.

The reaction temperature will affect the response signal of the biosensor. Different temperatures from 4 °C to 45 °C were tested. As shown in Fig. 2B, with the increase of the reaction temperature from 4 to 37 °C, the absorbance intensity increased accordingly. By the further increase of the temperature, the signal will decrease (blue histogram). On the other hand, the conformation of HP will be changed in relatively high temperature, which thus increased the background signal (black histogram). Additionally, Exo III might degrade the hairpin structure DNA at high temperature. Considering the best *S/N* ratio (red line), 25 °C was selected as the optimal reaction temperature.

As another important parameter, the incubation time of Exo III is also optimized. As shown in Fig. 2C, in the presence of 10 nM AFB1, the colorimetric signal gradually increased with the increase of the incubation time, and reached its plateau at 40 min (blue line), which demonstrated that the inaccessible G-rich fragment in HP almost

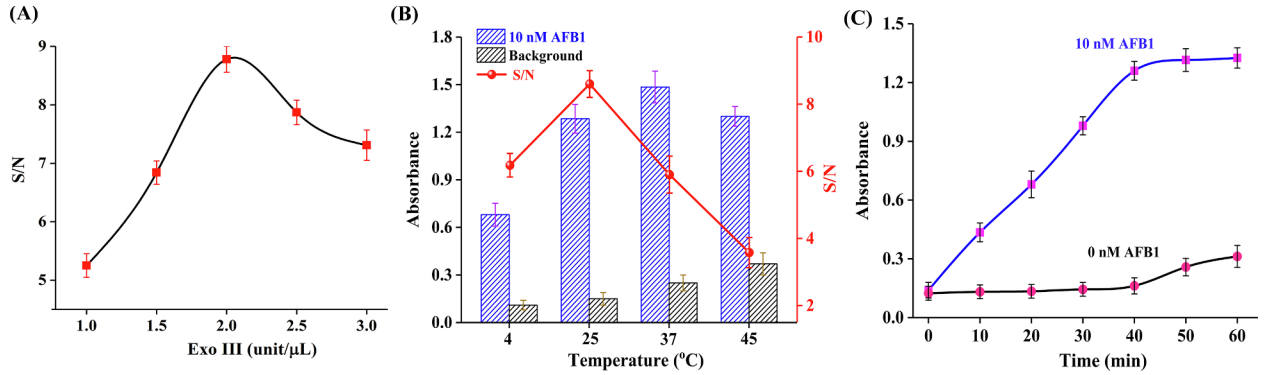

Fig. 2. (A) Effect of Exo III concentration on the performance of the colorimetric assay. AFB1 concentration, 10 nM. Reaction temperature, 25 °C. Exo III incubation time, 40 min. (B) Effect of reaction temperature on the performance of the colorimetric assay. The blue and black histograms represent the peak intensity of the reaction solution with and without 10 nM AFB1, respectively. The red line depicts the *S/N* ratio. Incubation time, 40 min. Exo III concentration, 2 unit/μL. (C) Effect of incubation time of Exo III on the performance of the colorimetric assay with 10 nM AFB1 (blue line) or without AFB1 (black line). Reaction temperature, 25 °C. Exo III concentration, 2 unit/μL. The error bars represent the standard deviation of three independent measurements. (For interpretation of the references to color in this figure legend, the reader is referred to the web version of this article.)

became free to form the active DNAzyme. However, gradual increase in background signal can be observed along with the incubation time extension (black line). To obtain the best detection results, 40 min was chosen as the optimal incubation time.

3.4. Sensing performance for AFB1 detection

Under optimal assay conditions, the sensing performance of our developed naked-eye biosensor was investigated by using different concentrations of target AFB1. As depicted in Fig. 3A, as the concentration of AFB1 increases, the color of the solution gradually turns blue, which is in accord with the fact that a higher AFB1 concentration results in the generation of more free G-quadruplex DNAzymes. The absorbance spectra of the solution were also recorded and shown in Fig. 3B. The peak intensity at 650 nm as a function of AFB1 concentration was shown in Fig. 3C. The absorption peak intensity showed a good linearity with the logarithm of the concentration of AFB1 ranging from 1 pM to 100 nM (Fig. 3C, inset). The linear regression equation can be expressed as: $y = 0.252 \times +0.212$, in which y represents the peak intensity at 650 nm, X represents the logarithm of the concentration of AFB1. Significantly, the presence of as low as 1 pM target AFB1 can be observed easily by the naked eye. The detection limit of 1 pM is superior to the currently used AFB1 ELISA kits (e.g., LOD of 5 pg/mL for Diagnostic Automation Inc. cat. no. 5120-8; LOD of 0.05 ppb for MyBioSource Inc. cat. no. MBS846684; and LOD of 0.2 ng/mL for Sigma, cat. no. SE120001). Such high sensitivity can ascribe to the smart HP design, the specific cleavage activity of Exo III, and the continuous turnover capability of the autocatalytic DNA circuit for cyclic signal amplification. These results demonstrated that our proposed biosensor was efficient for ultrasensitive detection of trace level of AFB1 concentration.

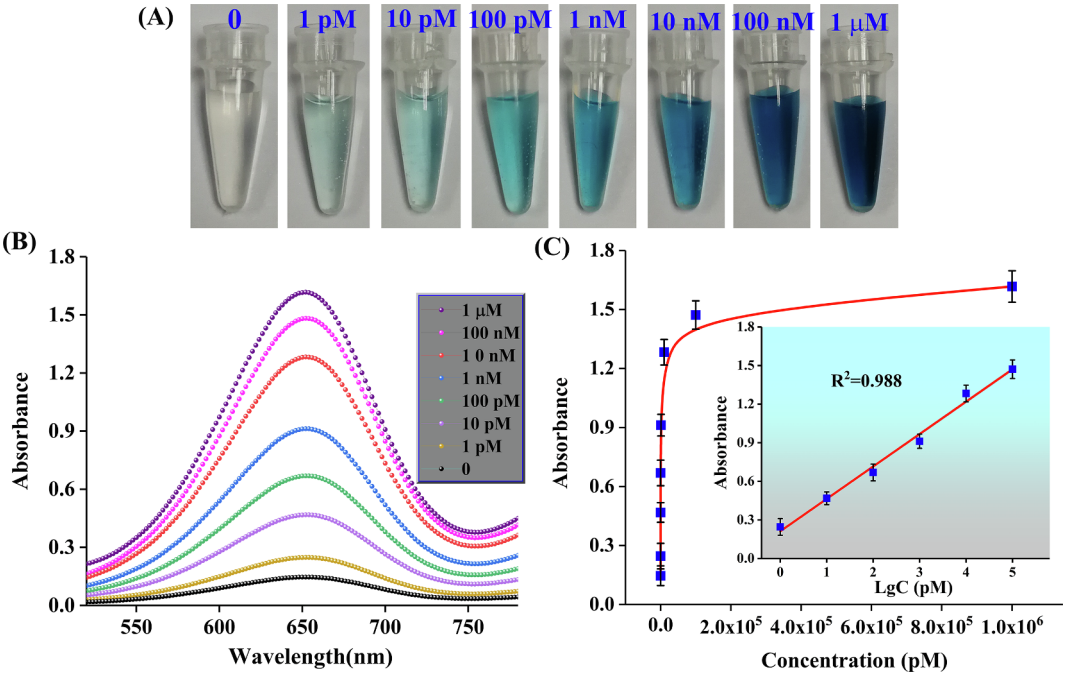

Fig. 3. (A) Photograph for the naked-eye detection of AFB1 at different concentrations. (B) The corresponding UV–vis absorption spectra. (C) Dependence of the absorption intensity at 650 nm on the target concentration. The inset shows the linear relationship between the peak intensity and the logarithm of AFB1 concentration ranging from 1 pM to 100 nM. The error bars represent the standard deviation of three independent measurements.

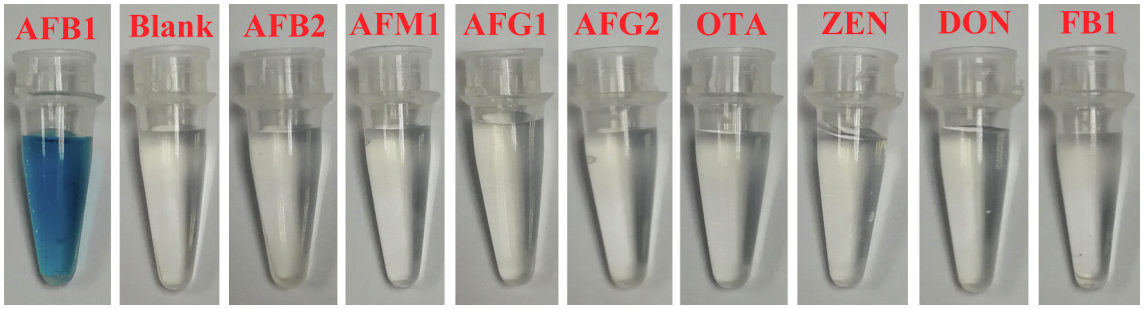

Fig. 4. Specificity of the developed biosensor for AFB1 against other mycotoxins. The concentration is 10 nM for AFB1 and 100 nM for other molecules.

Table 1
Recovery experiments of AFB1 determination in peanut samples.

Sample	Added (nM)	Found (mean[a] ± SD[b]) (nM)	Recovery (%)
Peanut sample 1	0.1	0.89 ± 0.06	89
Peanut sample 2	1	1.03 ± 0.14	103
Peanut sample 3	10	9.6 ± 0.37	96
Peanut sample 4	25	22.6 ± 1.58	90.4
Peanut sample 5	50	52.8 ± 4.52	105.6

[a] Mean of three determinations.
[b] SD, standard deviation.

3.5. Selectivity and real sample analysis

The specificity of the fabricated biosensor was also investigated by challenging this sensing system against other mycotoxins, for example, aflatoxin B2 (AFB2), aflatoxin M1 (AFM1), aflatoxin G1 (AFG1), aflatoxin G2 (AFG2), ochratoxin A (OTA), zearalenone (ZEN), deoxynivalenol (DON), and fumonisin (FB1). As depicted in Fig. 4., 10 nM AFB1 could cause the probe solution to be changed from colorless to blue color. Other non target analytes (100 nM) could not cause any obvious color change by comparison with the blank test. The results indicated that the proposed assay is good enough to selectively detect AFB1 from other control mycotoxins which may coexist in real samples. Such a high selectivity of this sensor can be attributed to the specific binding ability between the aptamer and the target.

To validate the applicability of the newly developed sensor in practical sample analysis, recovery experiments were performed by spiking AFB1 with different concentrations into the peanut samples. The measured data are listed in Table 1. Satisfactory values from 89% to 105.6% demonstrated that the possible interference from complex sample matrices was almost negligible. The recovery values are 103% and 105.6% for peanut samples two and five, respectively. The reason is that all values were obtained as an average of three repetitive determinations, and the standard deviation (SD) was different in those test. Thus, some recovery values are higher than 100% in the recovery experiments. The results indicated that the established biosensing system based on the autocatalytic DNA circuit could be applied for AFB1 determination in real agriculture products.

4. Conclusion

In summary, this work demonstrated a novel colorimetric assay for AFB1 detection based on an elegantly designed Exo-III assisted autocatalytic DNA circuit for cascade signal amplification. The presence of the target AFB1 triggers the continuous cleavage toward the hairpin DNA, resulting in the release of numerous caged G-quadruplex sequence. In the TMB-H_2O_2 sensing system, the results can be easily distinguished by the naked eye. The biosensor is ultrasensitive, enabling the naked-eye detection of AFB1 down to 1 pM without instrumentation. Besides, the proposed method is also highly selective for AFB1 against other mycotoxins. This sensing system is robust and had been used to detect the spiked AFB1 in peanut samples with satisfactory recovery. Moreover, this biosensor displays the unique advantages of simplicity in design, wash-free and label-free format, visible readout, and cost-effectiveness, making this biosensor especially suitable for in-field detection of AFB1 in resource restricted area. Importantly, our designed DNA circuit sensing system can be readily extended for other analytes detection by the simply substituting the target-specific molecular recognition sequence.

Acknowledgements

This work is supported by the NSFC (31671933), the Guangdong Natural Science Funds for Distinguished Young Scholars (2016A030306012), and the Local Innovative and Research Teams Project of Guangdong Pearl River Talents Program (2017BT01Z176).

Declaration of Competing Interest

None.

References

Arduini, F., Neagu, D., Pagliarini, V., Scognamiglio, V., Leonardis, M. A., Gatto, E., ... Moscone, D. (2016). Rapid and label-free detection of ochratoxin A and aflatoxin B1 using an optical portable instrument. *Talanta, 150*, 440–448.
Chen, J., Chen, S., & Li, F. (2017). Instrument-free visual detection of tetracycline on an autocatalytic DNA machine using a caged G-quadruplex as the signal reporter. *Chemical Communications, 53*, 8743–8746.
Chen, Y., Ding, L., Song, W., Yang, M., & Ju, H. (2016). Liberation of protein-specific glycosylation information for glycan analysis by exonuclease III-aided recycling hybridization. *Analytical Chemistry, 88*, 2923–2928.
Chen, J., Pan, J., & Chen, S. (2018). A label-free and enzyme-free platform with a visible output for constructing versatile logic gates using caged G-quadruplex as the signal transducer. *Chemical Science, 9*, 300–306.
Chen, J., Wen, J., Zhuang, L., & Zhou, S. (2016). An enzyme-free catalytic DNA circuit for amplified detection of aflatoxin B1 using gold nanoparticles as colorimetric indicators. *Nanoscale, 8*, 9791–9797.
Chen, J., Zhou, S., & Wen, J. (2015). Concatenated logic circuits based on a three-way DNA junction: A keypad-lock security system with visible readout and an automatic reset function. *Angewandte Chemie International Edition, 54*, 446–450.
Danesh, N. M., Bostan, H. B., Abnous, K., Ramezani, M., Youssefi, K., Taghdisi, S. M., & Karimi, G. (2018). Ultrasensitive detection of aflatoxin B1 and its major metabolite aflatoxin M1 using aptasensors: A review. *Trends in Analytical Chemistry, 99*, 117–128.
Eivazzadeh-Keihan, R., Pashazadeh, P., Hejazi, M., de la Guardia, M., & Mokhtarzadeh, A. (2017). Recent advances in nanomaterial-mediated bio and immune sensors for detection of aflatoxin in food products. *Trends in Analytical Chemistry, 87*, 112–128.
Gilbert, J., & Anklam, E. (2002). Validation of analytical methods for determining mycotoxins in foodstuffs. *Trends in Analytical Chemistry, 21*, 468–486.
Hao, N., Lu, J., Zhou, Z., Hua, R., & Wang, K. (2018). A pH-resolved colorimetric biosensor for simultaneous multiple target detection. *ACS Sensors, 3*, 2159–2165.
Hao, N., Zhang, Y., Zhong, H., Zhou, Z., Hua, R., Qian, J., ... Wang, K. (2017). Design of a dual channel self-reference photoelectrochemical biosensor. *Analytical Chemistry, 89*, 10133–10136.
Hosseini, M., Khabbaz, H., Dadmehr, M., Ganjali, M. R., & Mohamadnejad, J. (2015). Aptamer-based colorimetric and chemiluminescence detection of aflatoxin B1 in foods samples. *Acta Chimica Slovenica, 62*, 721–728.
Huang, W., Zhang, H., Lai, G., Liu, S., Li, B., & Yu, A. (2019). Sensitive and rapid aptasensing of chloramphenicol by colorimetric signal transduction with a DNAzyme-functionalized gold nanoprobe. *Food Chemistry, 270*, 287–292.
Jo, E.-J., Mun, H., Kim, S.-J., Shim, W.-B., & Kim, M.-G. (2016). Detection of ochratoxin A (OTA) in coffee using chemiluminescence resonance energy transfer (CRET)

aptasensor. *Food Chemistry, 194*, 1102–1107.
Li, Q., Lu, Z., Tan, X., Xiao, X., Wang, P., Wu, L., ... Han, H. (2017). Ultrasensitive detection of aflatoxin B1 by SERS aptasensor based on exonuclease-assisted recycling amplification. *Biosensors and Bioelectronics, 97*, 59–64.
Lin, Y., Zhou, Q., Tang, D., Niessner, R., & Knopp, D. (2017). Signal-on photoelectrochemical immunoassay for aflatoxin B1 based on enzymatic product-etching MnO_2 nanosheets for dissociation of carbon dots. *Analytical Chemistry, 89*, 5637–5645.
Liu, S., Cheng, C., Liu, T., Wang, L., Gong, H., & Li, F. (2015). Highly sensitive fluorescence detection of target DNA by coupling exonuclease-assisted cascade target recycling and DNAzyme amplification. *Biosensors and Bioelectronics, 63*, 99–104.
Liu, S., Lin, Y., Wang, L., Liu, T., Cheng, C., Wei, W., & Tang, B. (2014). Exonuclease III-aided autocatalytic DNA biosensing platform for immobilization-free and ultrasensitive electrochemical detection of nucleic acid and protein. *Analytical Chemistry, 86*, 4008–4015.
Lu, L., Su, H., & Li, F. (2017). Ultrasensitive homogeneous electrochemical detection of transcription factor by coupled isothermal cleavage reaction and cycling amplification based on exonuclease III. *Analytical Chemistry, 89*, 8328–8334.
Lv, L., Li, D., Cui, C., Zhao, Y., & Guo, Z. (2017). Nuclease-aided target recycling signal amplification strategy for ochratoxin A monitoring. *Biosensors and Bioelectronics, 87*, 136–141.
Ma, Y., Mao, Y., Huang, D., He, Z., Yan, J., Tian, T., ... Yang, C. (2016). Portable visual quantitative detection of aflatoxin B1 using a target-responsive hydrogel and a distance-readout microfluidic chip. *Lab on a Chip, 16*, 3097–3104.
Sabet, F. S., Hosseini, M., Khabbaz, H., Dadmehr, M., & Ganjali, M. R. (2017). FRET-based aptamer biosensor for selective and sensitive detection of aflatoxin B1 in peanut and rice. *Food Chemistry, 220*, 527–532.
Shim, W., Kim, M. J., Mun, H., & Kim, M. (2014). An aptamer-based dipstick assay for the rapid and simple detection of aflatoxin B1. *Biosensors and Bioelectronics, 62*, 288–294.
Taghdisi, S. M., Danesh, N. M., Ramezani, M., & Abnous, K. (2018). A new amplified fluorescent aptasensor based on hairpin structure of G-quadruplex oligonucleotide-aptamer chimera and silica nanoparticles for sensitive detection of aflatoxin B1 in the grape juice. *Food Chemistry, 268*, 342–346.
Wang, C., Qian, J., An, K., Ren, C., Lu, X., Hao, N., ... Wang, K. (2018). Fabrication of magnetically assembled aptasensing device for label-free determination of aflatoxin B1 based on EIS. *Biosensors and Bioelectronics, 108*, 69–75.
Wang, Z., Wang, L., Zhang, Q., Tang, B., & Zhang, C. (2018). Single quantum dot-based nanosensor for sensitive detection of 5-methylcytosine at both CpG and non-CpG sites. *Chemical Science, 9*, 1330–1338.
Wang, Z., Yu, H., Han, J., Xie, G., & Chen, S. (2017). Rare Co/Fe-MOFs exhibiting high catalytic activity in electrochemical aptasensors for ultrasensitive detection of ochratoxin A. *Chemical Communications, 53*, 9926–9929.
Wang, Y., Zhao, G., Li, X., Liu, L., Cao, W., & Wei, Q. (2018). Electrochemiluminescent competitive immunosensor based on polyethyleneimine capped SiO_2 nanomaterials as labels to release $Ru(bpy)_3^{2+}$ fixed in 3D Cu/Ni oxalate for the detection of aflatoxin B1. *Biosensors and Bioelectronics, 101*, 290–296.
Wu, L., Ding, F., Yin, W., Ma, J., Wang, B., Nie, A., & Han, H. (2017). From electrochemistry to electroluminescence: Development and application in a ratiometric aptasensor for aflatoxin B1. *Analytical Chemistry, 89*, 7578–7585.
Wu, Z., Xu, E., Jin, Z., & Irudayaraj, J. (2018). An ultrasensitive aptasensor based on fluorescent resonant energy transfer and exonuclease-assisted target recycling for patulin detection. *Food Chemistry, 249*, 136–142.
Wu, S., Zhang, B., Wang, F., Mi, Z., & Sun, J. (2018). Heating enhanced sensitive and selective electrochemical detection of Hg^{2+} based on T-Hg^{2+}-T structure and exonuclease III-assisted target recycling amplification strategy at heated gold disk electrode. *Biosensors and Bioelectronics, 104*, 145–151.
Xu, M., Gao, Z., Wei, Q., Chen, G., & Tang, D. (2016). Label-free hairpin DNA-scaffolded silver nanoclusters for fluorescent detection of Hg^{2+} using exonuclease III-assisted target recycling amplification. *Biosensors and Bioelectronics, 79*, 411–415.
Zhang, Z., Li, Y., Li, P., Zhang, Q., Zhang, W., Hu, X., & Ding, X. (2014). Monoclonal antibody-quantum dots CdTe conjugate-based fluoroimmunoassay for the determination of aflatoxin B1 in peanuts. *Food Chemistry, 146*, 314–319.
Zhang, K., Ren, T., Wang, K., Zhu, X., Wu, H., & Xie, M. (2014). Sensitive and selective amplified visual detection of cytokines based on exonuclease III-aided target recycling. *Chemical Communications, 50*, 13342–13345.
Zhao, Y., Huang, J., Ma, L., & Wang, F. (2017). Development and validation of a simple and fast method for simultaneous determination of aflatoxin B 1 and sterigmatocystin in grains. *Food Chemistry, 221*, 11–17.
Zhou, Z., Hao, N., Zhang, Y., Hua, R., Qian, J., Liu, Q., ... Wang, K. (2017). A novel universal colorimetric sensor for simultaneous dual target detection through DNA-directed self-assembly of graphene oxide and magnetic separation. *Chemical Communications, 53*, 7096–7099.
Zitomer, N., Rybak, M. E., Li, Z., Walters, M. J., & Holman, M. R. (2015). Determination of aflatoxin B1 in smokeless tobacco products by use of UHPLC-MS/MS. *Journal of Agricultural and Food Chemistry, 63*, 9131–9138.